Nanoscale

PAPER

View Article Online
View Journal

Solution-processed copper–nickel nanowire anodes for organic solar cells†

Cite this: DOI: 10.1039/c4nr01024h

Ian E. Stewart,‡[a] Aaron R. Rathmell,‡[a] Liang Yan,[b] Shengrong Ye,[a] Patrick F. Flowers,[a] Wei You[bc] and Benjamin J. Wiley*[a]

Received 24th February 2014
Accepted 10th April 2014

DOI: 10.1039/c4nr01024h

www.rsc.org/nanoscale

This work describes a process to make anodes for organic solar cells from copper–nickel nanowires with solution-phase processing. Copper nanowire films were coated from solution onto glass and made conductive by dipping them in acetic acid. Acetic acid removes the passivating oxide from the surface of copper nanowires, thereby reducing the contact resistance between nanowires to nearly the same extent as hydrogen annealing. Films of copper nanowires were made as oxidation resistant as silver nanowires under dry and humid conditions by dipping them in an electroless nickel plating solution. Organic solar cells utilizing these completely solution-processed copper–nickel nanowire films exhibited efficiencies of 4.9%.

1. Introduction

It's been noted that a solar energy conversion system cannot cost much more than ~10 times the cost of paint, or ~$10 per m^2, if it is to be cost-competitive with fossil fuels.[1,2] However, indium tin oxide (ITO), the transparent conductor used for solution-coatable organic photovoltaics (OPVs), by itself costs between $20–$90 per m^2.[3] Making the cost of OPVs competitive with fossil fuels will require transparent conductive paint that costs ~10 times less than ITO.

The high cost of ITO arises from several factors. Indium is a fairly rare and expensive (~$600 per kg) element, with an abundance in the earth's crust close to that of Ag (0.05 ppm).[4,5] ITO film is manufactured with a sputtering process that is fairly slow; the fastest film throughputs are around 0.01 m s^{-1}. In addition, less than 30% of the ITO sputtered from a target is deposited on the substrate, requiring a recycling infrastructure that adds additional cost.[4]

The high cost of ITO has driven a search for solution-coatable alternatives that can enable film throughputs up to 1000 times faster than ITO sputtering, near-complete transfer of the deposited material to the film, and comparable performance. Solution-coatable alternatives that have received extensive attention include conductive polymers,[6,7] carbon nanotubes,[8–10] graphene,[9,11] and metal nanowires.[12–16] Of these solution-coatable alternatives, only silver nanowires (Ag NWs) have demonstrated performance that exceeds that of ITO. As the coating process for Ag NWs is less costly and orders of magnitude faster than for ITO, Ag NWs will likely replace ITO as the transparent conductor of choice for applications that require relatively thick, high-conductivity (*i.e.*, high-cost) ITO, such as touch screens, organic light emitting diodes (OLEDs), and OPVs.[3,12,17,18] However, the price and abundance of Ag is similar to that of In.[4,5]

Copper is 6% less conductive than silver, but it is 1000 times more abundant and 100 times less expensive.[5,19] Thus, replacing Ag NWs with copper nanowires (Cu NWs) should offer comparable levels of performance at lower cost. One disadvantage of Cu NWs relative to Ag NWs is that they have a greater potential to oxidize, which reduces the conductivity of the film. Although films of Ag NWs can be heated in air to sinter them together at the contacts, and thereby reduce the contact resistance between nanowires, the fact that Cu NWs are covered with a layer of copper oxide prevents them from sintering together in air. Instead, it has been necessary to anneal Cu NW films under hydrogen in order for the films to obtain performance comparable to that of Ag NWs.[15,20–22] Despite the lower cost of Cu NWs, this lack of stability and necessity of hydrogen annealing has hindered their wider use in practical applications.

The challenges associated with making Cu NW networks conductive and protecting them from oxidation are likely responsible for the fact that there are many articles exploring the use of Ag NWs as a replacement for ITO in solar cells,[12,13,23–26] but only one recent report on the use of solution-coated Cu NWs in an OPV.[27] In that work, following hydrogen annealing of the Cu NW film, the nanowire electrode was planarized with PEDOT:PSS. The authors noted that the processing conditions

[a]Department of Chemistry, Duke University, 124 Science Drive, Box 90354, Durham, North Carolina 27708, USA. E-mail: benjamin.wiley@duke.edu

[b]Department of Chemistry, University of North Carolina at Chapel Hill, Chapel Hill, North Carolina 27599, USA

[c]Curriculum in Applied Sciences and Engineering, University of North Carolina at Chapel Hill, Chapel Hill, North Carolina 27599, USA

† Electronic supplementary information (ESI) available. See DOI: 10.1039/c4nr01024h

‡ These authors contributed equally to this work.

had to be modified to prevent the degradation of the Cu NW film during coating of the acidic PEDOT:PSS suspension. The authors vacuum deposited the remaining layers onto this anode to create a bulk-heterojunction (BHJ) small-molecule organic solar cell with an efficiency of 3%. Although this work demonstrated that Cu NWs can be used as an anode in a solar cell, unprotected Cu NWs are clearly not well-suited for this purpose since they will gradually become non-conductive due to oxidation over a matter of months.[28]

In this work we demonstrate an all solution-phase process to coat Cu NWs to form a film, make this film conductive, and protect it against oxidation. After coating Cu NWs from an ink onto glass, the films were made conductive by simply dipping them in acetic acid. These films were then made relatively stable against further oxidation by dipping them in a Ni electroless plating solution. Copper–nickel nanowire (CuNi NW) films were then integrated into a solution-coated OPV to give a device efficiency of 4.9%.

2. Experimental

2.1. Materials and instrumentation

For all nanowire films, transmittance and absorption data were collected using a UV-vis-NIR spectrophotometer (Cary 6000i) and sheet resistance values were measured using a four-point probe (Signatone SP4-50045TBS). The data points in Fig. 1D, 2D and 4A are each an average of 5 probe measurements. Metal concentration measurements were completed using a Perkin Elmer 3100 atomic absorption spectrophotometer (AAS). Pressing was performed with a shop press (model H6233Z) from Grizzly Industrial. Plasma cleaning was performed with a Harrick Plasma PDC-001. Optical microscopy images were taken with an Olympus BX51 microscope. SEM (FEI XL30 SEM-FEG), TEM (FEI Tecnai G^2 Twin), and AFM (Digital Instruments Dimension 3100) images were taken at the Shared Materials Instrumentation Facility at Duke University. Humidity chamber measurements were made in a Test Equity 200H Series temperature/humidity chamber at 85 °C/85 RH. Photovoltaic performance was characterized with a solar simulator (Oriel 91160, 300 W) under AM1.5 global one sun (100 mW cm^{-2} calibrated by a NREL certified standard silicon cell) at room temperature in a glove box. Current density *vs.* potential (*J–V*) curves were recorded with a Keithley 2400 digital source meter. The incident photon-to-current conversion efficiency (IPCE) measurements were carried out under monochromatic illumination (Oriel Cornerstone 260 1/4 m monochromator equipped with an Oriel 70613NS QTH lamp), and the calibration of the incident light was performed with a monocrystalline silicon diode.

2.2. Preparation of nanowire films

Copper nanowires ($L = 20 \pm 5$ μm, $D = 67 \pm 15$ nm) were synthesized by previously reported methods and donated by NanoForge Corp.[20] To separate the nanowires (1.4 mg mL^{-1} copper) from their storage solution of polyvinylpyrrolidone (PVP, 1 wt% in DI water, Aldrich) and diethylhydroxylamine (DEHA, 1 wt% in DI water, Aldrich), several purification steps were required. First, an aliquot (1 mL) of nanowires was collected and centrifuged at 2000 rpm for 5 minutes followed by decantation of the PVP–DEHA supernatant. The nanowire aggregates were then washed three times with DEHA (1 mL, 3 wt % in DI water) to remove the remaining PVP. Next, the nanowires were washed with 190 proof ethanol (1 mL, Koptec) to extract any residual water. The nanowires were then washed with an ink formulation consisting of 0.06 g nitrocellulose (Scientific Polymer) dissolved in 2.94 g acetone (EMD) with subsequent addition of 3 g ethanol (Pharmaco-Aaper), 0.5 g ethyl acetate (Aldrich), 1 g pentyl acetate (Aldrich), 1 g isopropanol (BDH), and 1.7 g toluene (Aldrich). The suspension was briefly vortexed and sonicated (<5 seconds) between washing steps.

Prior to preparing the Cu NW transparent electrodes, the glass substrates (3 in × 1 in microscope slides, VWR) were sonicated in acetone for ten minutes and transferred to isopropanol to remove surface contaminants. The slides were wiped dry with a kimwipe and blown dry under air immediately prior to nanowire deposition. Following decantation of the ink wash supernatant, a small amount (0.3 mL) of the ink was added to the nanowires resulting in a final Cu NW concentration of ~4.5 mg mL^{-1}. This suspension was vortexed to disperse the nanowires in the ink, and 35 μL was pipetted in a line across the top of the glass slide. A Meyer rod (Gardco #13) was then quickly (<1 second) drawn down the slide by hand to evenly spread the nanowire coating. The amount of ink added to the nanowires can be adjusted to vary the Cu NW concentration, and thus the transmittance and conductivity of the resulting film.

The slides coated with Cu NWs were dried in air for 10 minutes at 80 °C. Once the slides returned to room temperature, they were dipped in glacial acetic acid (Aldrich) for 2 seconds (Fig. 1A), dried under N_2 gas, and placed in an 80 °C oven for 45 seconds. Following four cycles of this procedure, the slides were allowed to cool to room temperature and then dipped in acetic acid and dried under N_2 twice more without additional oven drying. In some cases the slides were pressed at 80 bar at room temperature for one minute between glass slides functionalized with 1*H*,1*H*,2*H*,2*H*-perfluorooctyltriethoxysilane (Aldrich). To perform this functionalization, the slides were first plasma cleaned in air at a pressure of 0.8 to 0.93 mbar for 1 minute and placed in a dessicator under vacuum overnight along with an open vial containing 1 drop of 1*H*,1*H*,2*H*,2*H*-perfluorooctyltriethoxysilane.

For the Cu NW films annealed under H_2, the films were coated from the ink and dried in the oven as above. Instead of an acetic acid dip, the films were plasma cleaned under forming gas (95% N_2, 5% H_2) for 10 minutes at a pressure of 600 to 700 mTorr to remove residual organic material from the electrodes. Next, the electrodes were heated to 175 °C in a tube furnace under constant H_2 flow (600 mL min^{-1}) for 30 minutes to eliminate the remaining nitrocellulose and anneal the nanowires together.[20]

Silver nanowires were synthesized following previously published methods to give nanowires with dimensions of $L = 15 \pm 3$ μm and $D = 63 \pm 7$ nm.[29,30] Electrodes of Ag NWs were

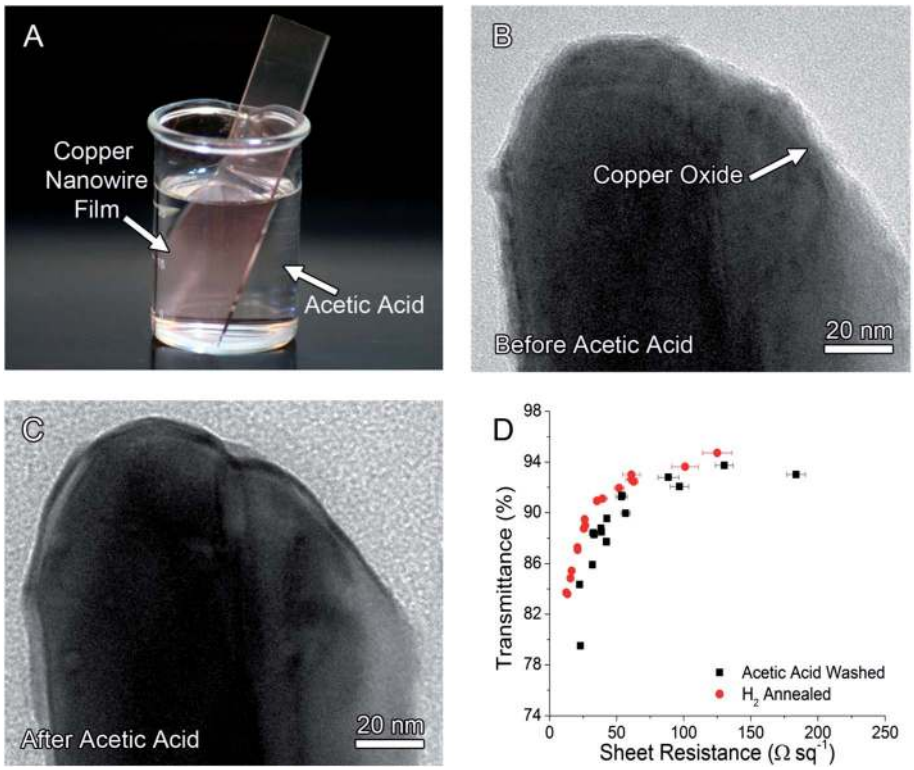

Fig. 1 (A) Cu NW film coated on a glass slide immersed in glacial acetic acid. TEM images of the same Cu NW (B) before and (C) after acetic acid treatment. (D) Plot of transmittance *vs.* sheet resistance for Cu NW films after annealing under H_2 at 175 °C or after the acetic acid treatment.

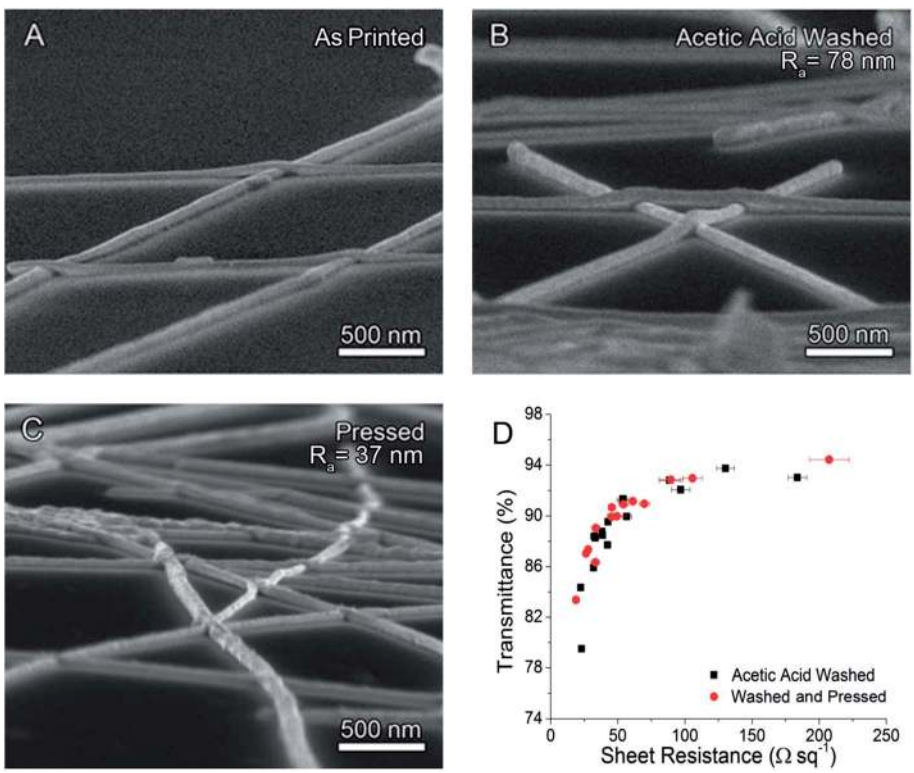

Fig. 2 SEM images of Cu NWs (A) as deposited, (B) washed with acetic acid, and (C) after pressing at 80 bar. (D) Plot of transmittance *vs.* sheet resistance of acetic acid washed Cu NW films before and after pressing.

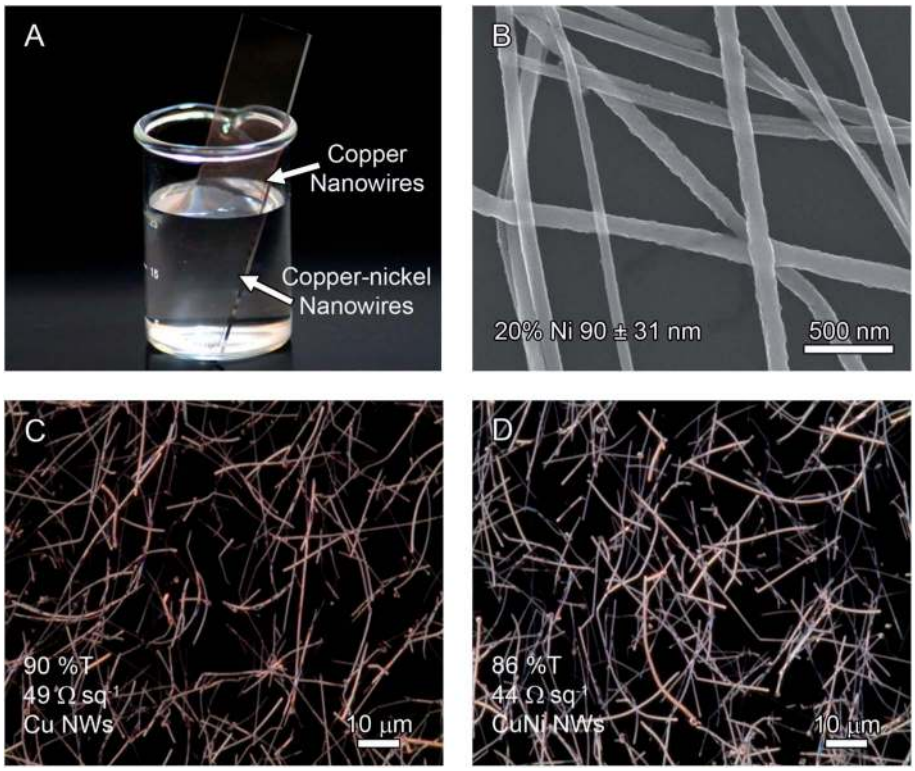

Fig. 3 (A) Cu NW film immersed in a nickel plating solution. (B) SEM image of CuNi NWs. Dark field optical microscope images of Cu NWs before (C) and after (D) Ni plating.

prepared in the same manner as Cu NW electrodes. After centrifuging and decanting the water from the nanowires, two rinses of ethanol were performed to ensure water removal. The Ag NWs were washed with the ink formulation, dispersed in ink, and coated onto glass slides *via* a Meyer rod. In order to remove any remaining organic material, the films were plasma cleaned under forming gas (95% N_2, 5% H_2) at a pressure of 600–700 mTorr for 10 minutes.

2.3. Electroless nickel plating

The nickel plating bath was prepared by heating 30 mL of DI water to 75 °C while stirring at 225 rpm. $Ni(NO_3)_2$ (0.1 M, 200 μL, Alfa Aesar) and hydrazine (35% weight, 150 μL, Aldrich) were added to the DI water after it reached the desired temperature. The Cu NW electrodes were then dipped into a 0.8 mM Pd^{2+} activation solution (10 mg sodium tetrachloropalladate from Aldrich in 40 g 190 proof ethanol from Koptec) for 20 seconds and immediately transferred to the Ni plating solution for various plating times. The amount of Ni deposited on the Cu NWs was measured by dissolving the CuNi films in concentrated nitric acid, and measuring the ratio of Ni to Cu with an AAS. By plotting the ratio of nickel to copper in the nanowires *versus* time in the plating bath, the amount of Ni plated onto the Cu NWs could be estimated and controlled (Fig. S1†). To prepare samples for the humidity chamber, the conductive films were first cut into 2.54 cm × 1 cm glass slides and silver paste was applied in strips to outline a 1 cm × 1 cm square. Next, the samples were inserted into the humidity chamber and the silver paste was connected through the silicone port plug of the chamber to a multimeter.

2.4. Measurement of Pd content and cost

Three Cu NW slides were treated with glacial acetic acid and pressed at 80 bar for 1 minute to a final transmittance of 91.5%. Each slide was then separately dipped into the Pd^{2+} activation solution described above for 20 seconds. The Pd-coated Cu NWs were then scraped off of the slides with a razor blade and collected in a vial. Aqua regia (0.5 mL) was added to dissolve the NWs and this solution was diluted to 12.5 mL with deionized water. The ratio of the mass of Cu to Pd was determined by AAS to be 10.2, and the cost of Pd was calculated to be \$0.13 per m^2 (Table S1†).

2.5. Fabrication of BHJ OPV electrodes

For the reference device on ITO-coated glass (Thin Film Devices, Inc.), a pre-patterned ITO glass substrate was cleaned with ultrasonication in deionized water, acetone, and isopropanol for 15 minutes each. The substrates were dried under a stream of nitrogen and then treated with UV–ozone for 15 minutes. A dispersion of the hole transport polymer, poly(3,4-ethylenedioxythiophene):poly(styrenesulfonate) (PEDOT:PSS) (AI 4083 Heraeus) was mixed with ethylene glycol (EG, J.T. Baker) in a 9 : 1 PEDOT:EG ratio by weight, and Zonyl FSO-100 (Aldrich, 5 mg Zonyl FSO-100 in 1 mL of a 9 : 1 PEDOT:PSS to EG mixture). The fluorosurfactant enhances the coverage of the polymer onto

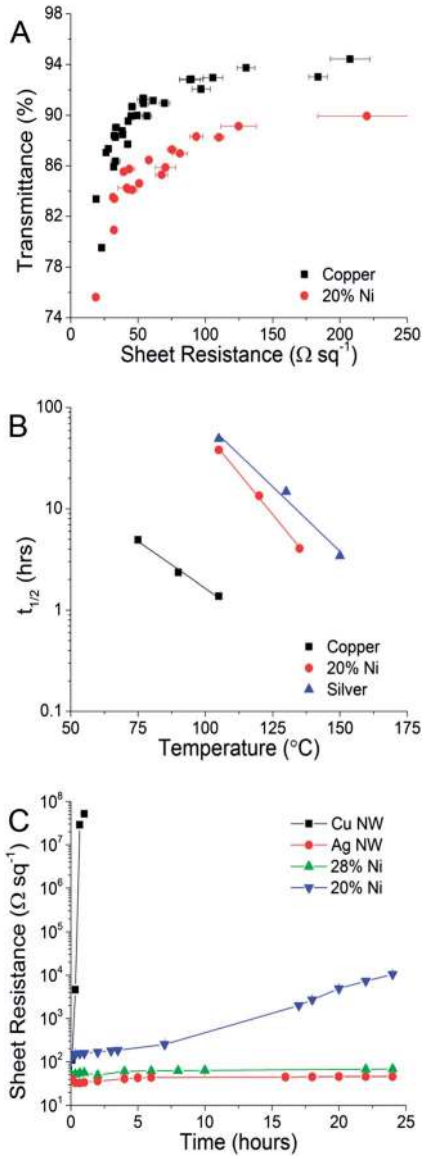

Fig. 4 (A) Transmittance *versus* sheet resistance for Cu NWs before and after nickel plating. (B) Modified Arrhenius plot of the time required for the sheet resistance to double *versus* temperature for films of Cu, 20% CuNi, and Ag NWs. (C) Sheet resistance change over 24 hours for Cu NWs, CuNi NWs (20% and 28% Ni) and Ag NWs under humid conditions (85 °C/85 RH).

the films.[31] Doping PEDOT:PSS with EG improves the conductivity of the polymer.[32,33] This mixture was then filtered through a 0.45 μm polyvinylidene fluoride filter, spun-cast onto the clean ITO substrates at 4000 rpm for 60 seconds, and baked at 130 °C for 15 minutes to give a film with a thickness of 40 nm.

The mixture of PEDOT:PSS, EG, and Zonyl was utilized as prepared for the CuNi NW films, but was diluted in a 2 : 1 ratio with DI water for the Ag NWs because doing so resulted in higher device efficiencies. The mixture was spin coated three times (4000, 2500, 4000 rpm for 1 minute each) onto pressed (80 bar, 1 minute) nanowire slides and dried under vacuum for 30 minutes. This processing resulted in film thicknesses of 52 nm and 26 nm for the undiluted and diluted EG–PEDOT:PSS, respectively.

To create the OPV active layer, previously synthesized PBnDT-FTAZ (benzo[1,2-*b*:4,5-*b*′]dithiophene (BnDT), fluorinated 2-alkyl-benzo[*d*][1,2,3]triazole (FTAZ)), and phenyl-C_{61}-butyric acid methyl ester (PCBM) were blended together and dissolved in 1,2,4-trichlorobenzene (30 mg mL^{-1} polymer) at 120 °C overnight.[34] The hot solution was passed through a 1 μm poly(tetrafluoroethylene) (PTFE) filter, spin coated (1 minute, 500 rpm) on the previously prepared PEDOT-coated substrates, and dried under vacuum for 20 minutes. Finally, the metal electrode (Ca 30 nm/Al 100 nm) was thermally evaporated onto the PBnDT-FTAZ:PCBM layer under vacuum (2×10^{-6} mbar) to complete the device.

3. Results and discussion

3.1. Preparation of conductive Cu NW films

Fig. 1A depicts the dipping of a Cu NW film into glacial acetic acid to remove copper oxide and the nitrocellulose left over from the ink from which the nanowires were coated. This simple procedure was inspired by previous reports that acetic acid can selectively remove copper oxides from the surface of copper without etching the underlying copper.[35] The experimental procedure described here has been optimized to minimize the resistance of the Cu NW film without damaging the nanowires or washing them off the substrate. Fig. 1B and C show TEM images of the same Cu NW taken before and after acetic acid treatment. The 2–3 nm-thick layer of copper oxide present in Fig. 1B is absent following the acetic acid treatment, but the underlying Cu NW appears unscathed. In addition to removing copper oxide, the glacial acetic acid removes nitrocellulose, the film former, from the substrate. The nitrocellulose can be observed as a white coating on the slide after the first dip in acetic acid. The white coating disappears after subsequent acetic acid dips, and remains as a residue in the beaker used for the acetic acid wash after the acetic acid evaporates.

Fig. 1D compares the transmittance (%T, $\lambda = 550$ nm) and sheet resistance (R_s) of Cu NW films that underwent the acetic acid treatment with those that underwent the plasma cleaning and annealing under H_2 at 175 °C. This comparison shows that the two methods obtain comparable film performance, with the H_2 annealing obtaining slightly better performance than the acetic acid treatment. We believe this difference is due to the fact that, while both methods eliminate copper oxides from the surface of the nanowire, the elevated temperature during H_2 annealing provides additional energy for the Cu NWs to sinter together and reduce contact resistance. Given that one would expect very little sintering to take place over the course of the acetic acid treatment, it is somewhat surprising that the acetic acid treatment can obtain values that are nearly equivalent to those obtained with annealing under H_2.

Mechanical pressing of nanowire films has previously been shown to decrease the sheet resistance of a Ag NW network, presumably by increasing the contact area between nanowires, and decreasing the contact resistance.[27,36–38] Thus it seems logical that the application of mechanical pressing after the acetic acid treatment might improve the performance of the

electrode to be comparable to the performance of a Cu NW film annealed under H_2. The SEM images in Fig. 2A and B show there is no discernable difference in the morphology of the Cu NW film before and after acetic acid treatment. After pressing the wires at 80 bar for 1 minute (Fig. 2C), the junctions between the nanowires appear to be fused together and the average surface roughness (R_a) decreases from 78 nm to 37 nm. However, a graph of $\%T$ *vs.* R_s before and after pressing (Fig. 2D) shows there is no improvement in performance after pressing. This is due to the fact that both the sheet resistance and the transmittance of the film decrease after pressing. For example, for a Cu NW film treated with acetic acid with an initial sheet resistance of 89 Ω sq^{-1} at 93% T, the sheet resistance and transmittance decreased to 61 Ω sq^{-1} and 91% T after pressing. The decrease in $\%T$ is likely due to flattening of the nanowires during the pressing process, which increases the area coverage of the nanowires, and decreases the light transmitted through the open areas of the network. Indeed, the Cu NWs appear to be more cylindrical in Fig. 2B, and somewhat more rectangular and flattened in Fig. 2C. Lowering or increasing the applied pressure relative to 80 bar did not result in any improved optoelectronic performance (see Fig. S1A†). Fig. S1B† shows the flattening of the nanowires was more pronounced at 160 bar than at 80 bar.

3.2. Electroless nickel plating

In order to protect the Cu NWs from oxidation, we have previously demonstrated the electroless plating of nickel onto the nanowires while they are dispersed in solution,[28] as well as the electroplating of nickel onto the nanowires after they are deposited on a film.[39] Electroplating Ni onto Cu NWs after film formation avoids laborious centrifugation and washing steps, eliminates ethylene glycol waste, and prevents the aggregation of NWs due to the magnetic attraction between CuNi NWs in solution. However, electroplating is somewhat more complicated in that it requires the use of a current source, and is difficult to apply uniformly over a large area due to the resistance of the nanowire film. Here we explore a third method, electroless plating of nickel onto copper nanowire films that offers the advantages of both previous methods with few of the disadvantages.

Following acetic acid treatment, the Cu NW electrodes were briefly dipped into an activation solution containing Pd^{2+} before being transferred to a nickel plating solution (Fig. 3A). Activation of the surface of Cu with Pd has previously been shown to facilitate the plating of Ni onto a Cu surface.[40,41] We see no plating of Ni onto the Cu NWs if they are not first exposed to Pd^{2+}. Although Pd is not an abundant, inexpensive element, so little of the Pd is actually incorporated into the nanowires (0.00482 g m^{-2}) that the contribution of the cost of Pd to the cost of the nanowire films is less than two orders of magnitude smaller than the cost of ITO film ($0.13 per m^2, see Table S1†).

A linear relationship between the time spent in the nickel solution and the amount of nickel deposited on the Cu NW network is shown in Fig. S2.† After 12.5 minutes in the plating solution, the diameter of the resulting CuNi NWs increased from 67 ± 15 nm to 90 ± 31 nm (Fig. 3B). Dark field optical microscope images of the nanowire network before and after 20% nickel plating (Fig. 3C and D) show that the color of the nanowires changed from reddish to grey. The nickel coating resulted in a small decrease in sheet resistance, but about a 4% drop in the transmittance (at $\lambda = 550$ nm). This drop in transmittance is consistent with previous results, and is due to the increase in the diameter of the nanowires after nickel coating.[28] Fig. 4A shows a graph of transmittance ($\lambda = 550$ nm) *versus* sheet resistance before and after the nickel coating.

Fig. 4B shows coating the Cu NWs with 20% Ni gives them a resistance to oxidation comparable to Ag NWs. This plot shows the time required for the sheet resistance of nanowire films of comparable transmittance (85–87% T) to double ($t_{1/2}$) after being placed in a dry oven heated to a given temperature (75–150 °C). For example, it takes about 1 h for the sheet resistance of a Cu NW film to double at 105 °C, but this increases to 38 h if the NWs are coated with 20% Ni. The stability of the nanowire films was also compared in a humidity chamber at 85 °C and 85 ± 3% RH (Fig. 4C). Under these conditions, Cu NW films became insulating in less than 1 h, 20% CuNi NWs were stable for <5 h, and 28% CuNi NWs exhibited a stability similar to Ag NW films.

3.3. CuNi NW solar cell performance

One of the obstacles to the replacement of ITO with nanowire films in OPVs is the greater surface roughness of nanowire electrodes.[42] The peak-to-valley surface roughness of nanowire electrodes coated from solution and treated with acetic acid (Fig. 2B) is slightly less than two nanowire diameters, or 104 nm. This surface roughness is nearly the same as the thickness of a typical polymer active layer. As a result, many of the OPV devices made with nanowire electrodes have exhibited small shunt resistances, and correspondingly low OPV efficiencies.[23,24,26,43,44]

One approach to making a smooth nanowire electrode involves transferring the nanowires from a donor substrate to a polymer, and in the process embedding them in the polymer.[45] In one case, this was accomplished by spin coating a polymer (polyacrylate) over a film of Ag NWs, photocuring the polymer film, and peeling away the polymer film to reveal a smooth (rms roughness < 5 nm) surface containing the nanowires embedded in the polymer film.[44] The best device made with this method exhibited an efficiency of 3.28%.[44] Peumans and co-workers achieved an efficiency of 4.2% by laminating Ag NWs into the surface of PEDOT:PSS.[42] However, transferring the nanowires from one substrate to another is quite difficult to do with high fidelity, and may result in low device yields in a production environment.

We have found that comparable or greater device efficiencies can be achieved by optimizing the coating process for PEDOT:PSS over the nanowire film. We have previously obtained device efficiencies of 2.8% and 2.5% on glass and PET, respectively, by coating a Ag NW film with a single coating of PEDOT:PSS with a thickness of 40 nm.[23] Since then, we have found that coating the nanowire film three times with

PEDOT:PSS mixed with EG and a fluorosurfactant allowed us to achieve device efficiencies nearly twice that of those obtained previously. As the current PEDOT:PSS coating is not much thicker than the ones used previously, we believe the reason for the increase in device efficiency from the three-step coating process is principally due to the fact that a more complete coating is achieved, thereby facilitating the transport of holes to the metallic nanowires while preventing device shorts and electron–hole recombination at the surface of the metal nanowires.

Fig. 5A and B show AFM images before and after CuNi NWs were coated with PEDOT:PSS. Prior to testing the CuNi NW electrodes in an OPV device, the films were pressed (80 bar, 1 minute) in an attempt to decrease the roughness of the nanowire network. A nickel concentration of 28% was chosen to increase the resistance of the nanowire film to oxidation. The R_a of the pressed CuNi NWs dropped from 52 nm to 18 nm after coating PEDOT:PSS onto the nanowires.

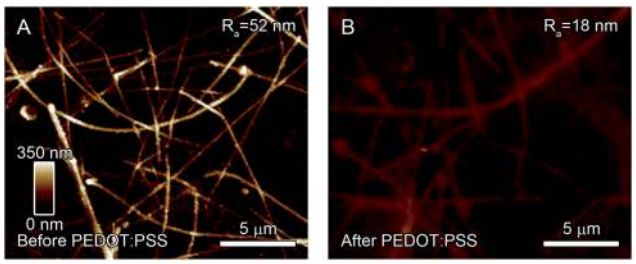

Fig. 5 AFM images of Cu NW films (A) before and (B) coating with PEDOT:PSS.

Fig. 6A is a schematic illustrating the layers of the finished device. FTAZ:PCBM denotes the blend of PBnDT-FTAZ and PCBM used as the active layer. This blend was chosen due to its previously demonstrated high performance in BHJ OPVs utilizing nanowires as the transparent electrode.[23] Films of Ag NWs (%$T = 76$, $R_s = 14\ \Omega\ sq^{-1}$) and CuNi NWs (%$T = 80$, $R_s = 36\ \Omega\ sq^{-1}$) were fabricated to have similar film properties to determine if the replacement of Ag with the lower-cost CuNi NWs would affect the performance of the OPV. Representative current–voltage curves for the devices are shown in Fig. 6B and the relevant photovoltaic characteristics are summarized in Table 1. Compared to the ITO reference, both nanowire based devices display lower short-circuit currents (J_{SC}; J at $V = 0$), lower fill factor (FF), and slightly lower open circuit voltages (V_{OC}; V at $J = 0$), resulting in lower device efficiencies.

Previous papers also show that the V_{OC} for OPVs using Ag NW films is lower than ITO films.[12,23–25] This has previously been attributed to the fact that Ag has a lower work function (4.3–4.7 eV)[46–48] than ITO (4.7–5.0 eV),[49–51] resulting in a

Table 1 Photovoltaic performance of the FTAZ BHJ solar cells

Anode	J_{SC} (mA cm^{-2})	V_{OC} (V)	FF (%)	η (%)
ITO	11.97	0.810	74.0	7.1
Ag NW	10.18	0.776	63.4	5.0
CuNi NW	9.98	0.767	63.5	4.9

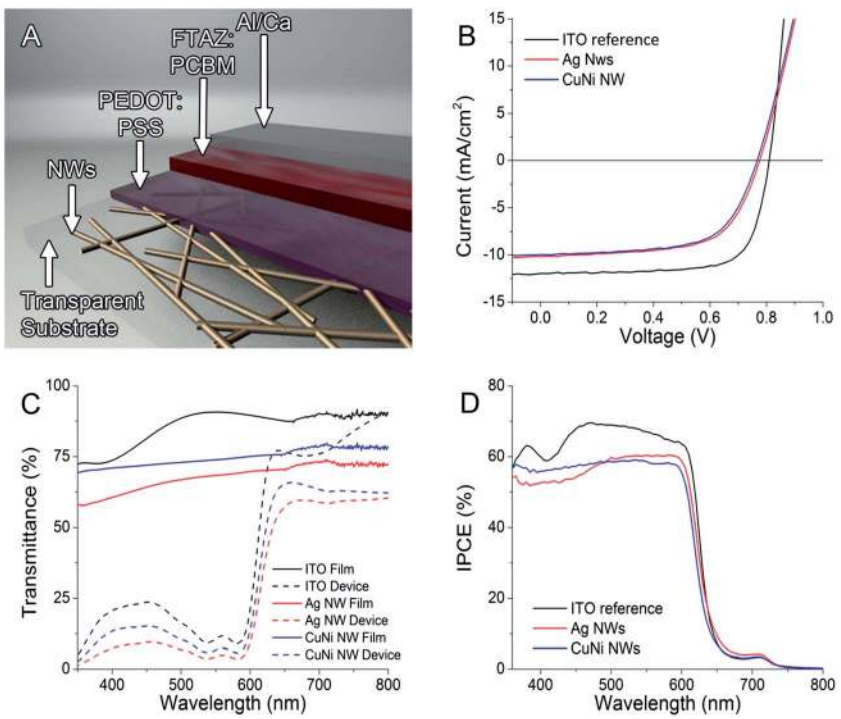

Fig. 6 (A) Diagram of the nanowire-based FTAZ BHJ solar cell. (B) Characteristic J–V curves of solar cells with ITO, Ag NWs, and CuNi NWs as the transparent electrode. (C) The transmittance of the transparent conducting films and respective devices *versus* wavelength. (D) IPCE *versus* wavelength curves of the FTAZ BHJ solar cells with ITO, Ag NW, and CuNi NW anodes under one sun condition (100 mW cm^{-2}).

greater barrier to the transport of holes out of the device.[23] Compared to our previous work in which the V_{OC} for OPVs using nanowire films as anodes was on average 59% of those obtained for ITO, the three step coating process has improved the V_{OC} to be 96% (Ag NWs) and 95% (CuNi NWs) that of the ITO reference. The slightly lower V_{OC} observed for nanowire films may be due to the fact that the coverage of PEDOT:PSS on the nanowires is not as uniform and pinhole-free as the coating of PEDOT:PSS on ITO.

The lower J_{SC} of the devices can be attributed to the lower transmittance of the Cu NW and Ag NW films relative to ITO. The J_{SC} of the nanowire-based devices is roughly 20% lower than the ITO-based device, which is roughly equivalent to the difference in the percent of incident light absorbed by the nanowire and ITO-based devices (see Table S2† and Fig. 6C). This inference is further supported by the correlation between the transmittance of the films and devices (Fig. 6C) with the incident photon to current efficiency (IPCE) of the devices (Fig. 6D). Thus the J_{SC} of the nanowire-based devices can likely be improved by improving the transmittance of the nanowire films at a given sheet resistance.[25,52]

4. Conclusion

We have shown that simply dipping Cu NW films in acetic acid makes them nearly as conductive as Cu NW films annealed under hydrogen. We have further introduced a film-based electroless nickel plating process that gives Cu NW films a stability comparable to Ag NW films, even under humid conditions. Finally, we have shown that BHJ OPVs using films of CuNi NWs as the transparent anode can achieve a device efficiency of 4.9%, nearly equivalent to the 5% efficiency of a BHJ OPV utilizing Ag NWs as the transparent anode.

By simplifying the processing of Cu NW films, we hope this work helps to remove existing hurdles to the wider practical application of Cu NWs. That being said, the simple coat and heat processing used for Ag NWs remains easier than the processing necessary for Cu NWs, so there is still room for further simplification of the processing steps.[13] In addition, although the CuNi device efficiency of 4.9% is relatively high compared to previous work, it is still lower than the 7.1% device efficiency obtained for the device based on ITO. This issue can likely be addressed by using films composed of nanowires with higher aspect ratios, which exhibit a higher transmittance at the same sheet resistance.[15,53]

Acknowledgements

This work was supported in part by the National Science Foundation's (NSF's) Research Triangle MRSEC (DMR-1121107), an NSF CAREER award (DMR-1253534), EMD Millipore, and NSF grant no. ECCS-1344745. I.E.S. and P.F.F. acknowledge support by a fellowship from the Graduate Certificate Program in Nanoscience at Duke University.

References

1 N. S. Lewis and D. G. Nocera, *Proc. Natl. Acad. Sci. U. S. A.*, 2006, **103**, 15729–15735.
2 C. Wadia, A. P. Alivisatos and D. M. Kammen, *Environ. Sci. Technol.*, 2009, **43**, 2072–2077.
3 C. J. M. Emmott, A. Urbina and J. Nelson, *Sol. Energy Mater. Sol. Cells*, 2012, **97**, 14–21.
4 D. C. U.S. Geological Survey, *Mineral Commodity Summaries, Indium*, U.S. Department of the Interior, Washington, 2013, p. 2074.
5 D. C. U.S. Geological Survey, *Mineral Commodity Summaries, Silver*, U.S. Department of the Interior, Washington, 2013, p. 2146.
6 S. Kirchmeyer and K. Reuter, *J. Mater. Chem.*, 2005, **15**, 2077–2088.
7 A. Elschner and W. Lövenich, *MRS Bull.*, 2011, **36**, 794–798.
8 Z. Wu, Z. Chen, X. Du, J. M. Logan, J. Sippel, M. Nikolou, K. Kamaras, J. R. Reynolds, D. B. Tanner, A. F. Hebard and A. G. Rinzler, *Science*, 2004, **305**, 1273–1276.
9 D. S. Hecht, L. B. Hu and G. Irvin, *Adv. Mater.*, 2011, **23**, 1482–1513.
10 C. Niu, *MRS Bull.*, 2011, **36**, 766–773.
11 S. Bae, H. Kim, Y. Lee, X. Xu, J.-S. Park, Y. Zheng, J. Balakrishnan, T. Lei, H. R. Kim, Y. I. Song, Y.-J. Kim, K. S. Kim, B. Ozyilmaz, J.-H. Ahn, B. H. Hong and S. Iijima, *Nat. Nanotechnol.*, 2010, **5**, 574–578.
12 J.-W. Lim, D.-Y. Cho, K. Eun, S.-H. Choa, S.-I. Na, J. Kim and H.-K. Kim, *Sol. Energy Mater. Sol. Cells*, 2012, **105**, 69–76.
13 M. Song, D. S. You, K. Lim, S. Park, S. Jung, C. S. Kim, D.-H. Kim, D.-G. Kim, J.-K. Kim, J. Park, Y.-C. Kang, J. Heo, S.-H. Jin, J. H. Park and J.-W. Kang, *Adv. Funct. Mater.*, 2013, **23**, 4177–4184.
14 J. Lee, P. Lee, H. Lee, D. Lee, S. S. Lee and S. H. Ko, *Nanoscale*, 2012, **4**, 6408–6414.
15 S. Ye, A. R. Rathmell, I. E. Stewart, Y.-C. Ha, A. R. Wilson, Z. Chen and B. J. Wiley, *Chem. Commun.*, 2014, **50**, 2562–2564.
16 H. Z. Guo, N. Lin, Y. Z. Chen, Z. W. Wang, Q. S. Xie, T. C. Zheng, N. Gao, S. P. Li, J. Y. Kang, D. J. Cai and D. L. Peng, *Sci. Rep.*, 2013, **3**, 8.
17 A. Kumar and C. Zhou, *ACS Nano*, 2010, **4**, 11–14.
18 L. Hu, H. Wu and Y. Cui, *MRS Bull.*, 2011, **36**, 760–765.
19 D. C. U.S. Geological Survey, *Mineral Commodity Summaries, Copper*, U.S. Department of the Interior, Washington, 2013, p. 2048.
20 A. R. Rathmell and B. J. Wiley, *Adv. Mater.*, 2011, **23**, 4798–4803.
21 A. R. Rathmell, S. M. Bergin, Y.-L. Hua, Z.-Y. Li and B. J. Wiley, *Adv. Mater.*, 2010, **22**, 3558–3563.
22 S. Ye, A. R. Rathmell, Y.-C. Ha, A. R. Wilson and B. J. Wiley, *Small*, 2014, **10**, 1771–1778.
23 L. Q. Yang, T. Zhang, H. X. Zhou, S. C. Price, B. J. Wiley and W. You, *ACS Appl. Mater. Interfaces*, 2011, **3**, 4075–4084.

24 D. S. Leem, A. Edwards, M. Faist, J. Nelson, D. D. C. Bradley and J. C. de Mello, *Adv. Mater.*, 2011, **23**, 4371–4375.
25 N. Yong-Jin, K. Seok-Soon, K. Tae-Wook and N. Seok-In, *Semicond. Sci. Technol.*, 2013, **28**, 125008.
26 W. Gaynor, J. Y. Lee and P. Peumans, *ACS Nano*, 2010, **4**, 30–34.
27 C. Sachse, N. Weiß, N. Gaponik, L. Müller-Meskamp, A. Eychmüller and K. Leo, *Adv. Eng. Mater.*, 2014, DOI: 10.1002/aenm.201300737.
28 A. R. Rathmell, M. Nguyen, M. F. Chi and B. J. Wiley, *Nano Lett.*, 2012, **12**, 3193–3199.
29 B. Wiley, Y. G. Sun and Y. N. Xia, *Langmuir*, 2005, **21**, 8077–8080.
30 S. M. Bergin, Y. H. Chen, A. R. Rathmell, P. Charbonneau, Z. Y. Li and B. J. Wiley, *Nanoscale*, 2012, **4**, 1996–2004.
31 M. Vosgueritchian, D. J. Lipomi and Z. Bao, *Adv. Funct. Mater.*, 2012, **22**, 421–428.
32 J. Ouyang, C. W. Chu, F. C. Chen, Q. Xu and Y. Yang, *Adv. Funct. Mater.*, 2005, **15**, 203–208.
33 J. Ouyang, Q. Xu, C.-W. Chu, Y. Yang, G. Li and J. Shinar, *Polymer*, 2004, **45**, 8443–8450.
34 S. C. Price, A. C. Stuart, L. Yang, H. Zhou and W. You, *J. Am. Chem. Soc.*, 2011, **133**, 4625–4631.
35 K. L. Chavez and D. W. Hess, *J. Electrochem. Soc.*, 2001, **148**, G640–G643.
36 T. Tokuno, M. Nogi, M. Karakawa, J. T. Jiu, T. T. Nge, Y. Aso and K. Suganuma, *Nano Res.*, 2011, **4**, 1215–1222.
37 J. H. Choi, J. P. Kar, D. Y. Khang and J. M. Myoung, *J. Phys. Chem. C*, 2009, **113**, 5010–5013.
38 L. B. Hu, H. S. Kim, J. Y. Lee, P. Peumans and Y. Cui, *ACS Nano*, 2010, **4**, 2955–2963.
39 Z. Chen, A. R. Rathmell, S. Ye, A. R. Wilson and B. J. Wiley, *Angew. Chem., Int. Ed.*, 2013, **52**, 13708–13711.
40 F. Z. Kong, X. B. Zhang, W. Q. Xiong, F. Liu, W. Z. Huang, Y. L. Sun, J. P. Tu and X. W. Chen, *Surf. Coat. Technol.*, 2002, **155**, 33–36.
41 J. F. Rohan, G. O'Riordan and J. Boardman, *Appl. Surf. Sci.*, 2002, **185**, 289–297.
42 W. Gaynor, G. F. Burkhard, M. D. McGehee and P. Peumans, *Adv. Mater.*, 2011, **23**, 2905–2910.
43 J. Y. Lee, S. T. Connor, Y. Cui and P. Peumans, *Nano Lett.*, 2008, **8**, 689–692.
44 Z. B. Yu, L. Li, Q. W. Zhang, W. L. Hu and Q. B. Pei, *Adv. Mater.*, 2011, **23**, 4453–4457.
45 X. Y. Zeng, Q. K. Zhang, R. M. Yu and C. Z. Lu, *Adv. Mater.*, 2010, **22**, 4484–4488.
46 M. Methfessel, D. Hennig and M. Scheffler, *Phys. Rev. B: Condens. Matter Mater. Phys.*, 1992, **46**, 4816–4829.
47 *CRC Handbook of Chemistry and Physics*, CRC Press, 2008.
48 R. E. Hummel, *Electronic Properties of Materials*, Springer-Verlag, New York, 3rd edn, 2001.
49 K. X. Steirer, P. F. Ndione, N. E. Widjonarko, M. T. Lloyd, J. Meyer, E. L. Ratcliff, A. Kahn, N. R. Armstrong, C. J. Curtis, D. S. Ginley, J. J. Berry and D. C. Olson, *Adv. Eng. Mater.*, 2011, **1**, 813–820.
50 E. L. Ratcliff, A. Garcia, S. A. Paniagua, S. R. Cowan, A. J. Giordano, D. S. Ginley, S. R. Marder, J. J. Berry and D. C. Olson, *Adv. Eng. Mater.*, 2013, **3**, 647–656.
51 M. D. Irwin, J. D. Servaites, D. B. Buchholz, B. J. Leever, J. Liu, J. D. Emery, M. Zhang, J. H. Song, M. F. Durstock, A. J. Freeman, M. J. Bedzyk, M. C. Hersam, R. P. H. Chang, M. A. Ratner and T. J. Marks, *Chem. Mater.*, 2011, **23**, 2218–2226.
52 S. K. Hau, H.-L. Yip, J. Zou and A. K. Y. Jen, *Org. Electron.*, 2009, **10**, 1401–1407.
53 R. M. Mutiso, M. C. Sherrott, A. R. Rathmell, B. J. Wiley and K. I. Winey, *ACS Nano*, 2013, **7**, 7654–7663.